Microporous and Mesoporous Materials xxx (xxxx) xxx–xxx

Contents lists available at ScienceDirect

Microporous and Mesoporous Materials

journal homepage: www.elsevier.com/locate/micromeso

Influence of exchange in NMR pore size/relaxation correlation experiments

Emilia V. Silletta, María B. Franzoni, Gustavo A. Monti, Rodolfo H. Acosta*

FaMAF-Universidad Nacional de Córdoba and IFEG-CONICET, 5016, Córdoba, Argentina

ARTICLE INFO

Keywords:
NMR methods
Molecular exchange
Pore surface relaxivity
Pore size distribution
Polymeric porous network

ABSTRACT

The influence of molecular exchange in porous polymeric systems on experiments that simultaneously correlate and determine pore length scales and surface relaxivities is studied. Pore length scales are determined by taking advantage of the internal field gradients generated by the difference in magnetic susceptibility between the polymer matrix and the contained water, namely the Decay Due to the Internal Field experiment. Transverse relaxation is codified in the detection period thus enabling correlation with the pore length. For the hierarchical very well connected porous polymer system, the considerable molecular exchange of water between different environments renders signals in the two-dimensional maps that make the determination of the surface relaxivity a complex problem.

1. Introduction

Nuclear magnetic resonance (NMR) has become a valuable tool over the last decades for the characterization of porous media. The ability to determine pore matrix characteristics through the measurement of restricted fluids enables not only the determination of average pore sizes, but also provides more valuable information such as liquid/surface interactions which play a fundamental role in applications such as oil extraction from reservoir rocks [1], catalysis [2] and liquid separation processes [3] among other examples. The general approach is to determine either relaxation time constants of confined liquids, which depend on the surface relaxivity and pore dimension, or restricted diffusion coefficients, which provide information on surface to volume (S/V) ratios and tortuosity [4]. Additionally, direct determination of pore sizes may be achieved by using the decay due to the internal field (DDIF) method, which relies on the decay of magnetization due to molecular diffusion in internal field gradients, generated by different magnetic susceptibilities present in a heterogeneous sample exposed to a magnetic field [5].

In the fast diffusion limit [6], transverse relaxation (T_2) depends on the surface to volume ratio, S/V, and the surface relaxivity ρ_2, via the relation:

$$\frac{1}{T_2} = \frac{1}{T_{2b}} + \frac{\rho_2 S}{V} \tag{1}$$

where T_{2b} is the bulk transverse relaxation time. Transverse relaxation times are usually recorded using the Carr-Purcell-Meiboom-Gill (CPMG) pulse sequence, where the decay of spin echoes during a train of π pulses is acquired [7,8]. For systems with a distribution of pore lengths, a distribution of decay rates is obtained by numerical inversion. In order to obtain the pore size distribution (PSD), the surface relaxivity must be known and pore geometry assumed. On the other hand, if the PSD is known a priori, ρ_2 provides valuable information about the liquid/surface interactions. While the PSD can in principle be determined by a variety of methods [9] such as optical ones, scattering or by mercury intrusion, often the system may undergo changes between the dry and swollen state or to be deformed by imposing high pressures. It is then desirable to perform all experiments in the same experimental conditions. For instance, Muncaci et al. [10] studied frequency dependent longitudinal surface relaxivity (by Fast Field Cycling NMR) in porous ceramics with varying degree of paramagnetic impurities, and determined the pore sizes by using the DDIF sequence at 0.5T.

However, it is preferable to obtain both the S/V ratio and relaxation times simultaneously, by the use of 2D experiments. Recently Luo et al. [11] introduced a method in which diffusion and relaxation are simultaneously encoded, and the time-dependent diffusion coefficient [12,13] is used to determine the S/V ratio, thus obtaining the surface relaxation from a single experiment. Assuming a distribution of spherical cavities, then the relaxation rates can be associated with the pore size d by expressing $\frac{\rho_i S}{V} = \frac{6\rho_i}{d}$. Liu et al. [14] combined a DDIF experiment with CPMG detection in order to simultaneously determine pore sizes and transverse relaxation in rock cores at 2MHz. They conclude that a single surface relaxivity parameter describes very well the whole system. The same strategy was applied for the determination of heterogeneity in the PSD [15] and also the different diffusion coefficients of water and oil were exploited as a filter during the DDIF encoding

* Corresponding author.
E-mail address: racosta@famaf.unc.edu.ar (R.H. Acosta).

http://dx.doi.org/10.1016/j.micromeso.2017.10.025
Received 12 December 2016; Received in revised form 25 April 2017; Accepted 13 October 2017

period [16].

In this work, we focus on the study of porous polymeric systems which present a hierarchical PSD [17]. These systems are characterized by presenting three recognizable different environments. A network of large pores which is fully interconnected with smaller voids which, in turn, present a superficial gel phase with a great amount of OH groups [18,19]. Additionally, these systems are stable both in the dry and swollen state, with porosities about 80%, which makes them ideal candidates for liquid separation process. We have previously reported a combination of 1D DDIF and CPMG results for the characterization of the surface relaxivities [20]. Remarkably the relaxivities were observed to change between different cavities. In the present work, we apply the 2D DDIF-CPMG strategy and show that for these systems cross-peaks due to exchange between different pores appear in the 2D maps. Therefore the surface relaxivity cannot be characterized by the usual linear dependence between pore size and relaxation.

2. Theoretical background

2.1. Molecular exchange determination

Molecular exchange due to diffusion between different pores is often carried out by relaxation-relaxation encoding. The T_2-T_2 exchange NMR is a technique widely used to study fluid dynamics within porous media [21,22]. In Fig. 1a a scheme of the pulse sequence is presented. The experiment measures the movement of a fluid between different environments and is visualized in a T_2-T_2 map generated by inverting the data solving Fredholm integrals of the first kind in 2D [23]. During the entire experiment, the fluid molecules can remain in their original environment or can migrate from one environment to another. In the former case, the magnetization signal will appear along the diagonal in the T_2-T_2 map, while in the latter case relaxation time coordinates will be a combination of different involved environments, and off-diagonal peaks will be observed.

2.2. DDIF-CPMG experiment

When a fluid is confined in a porous media and placed in an external magnetic field, internal magnetic field gradients arise due to the susceptibility contrast between the fluid and the solid matrix. The spatial distribution of this internal magnetic field will be determined by the structure of the porous medium. The liquid molecules inside the void spaces diffuse in the presence of these gradients with a resulting loss of signal. The idea behind the DDIF method is to establish a spin magnetization modulation that senses the spatial variation of the internal magnetic field within each individual pore [24]. The DDIF sequence consists of two individual experiments. A stimulated echo is used for pore size codification (Fig. 1b), where an initial encoding period t_e allows for a local field gradients mapping, each spin acquires a phase that is proportional to the local field $\Phi = \gamma B(r) t_e$, i.e. the internal field variation within a pore is encoded in the phase of spins. After the encoding period, the magnetization is rotated to the z-axis (no transverse relaxation) and diffusion through the internal field takes place during a period t_d.

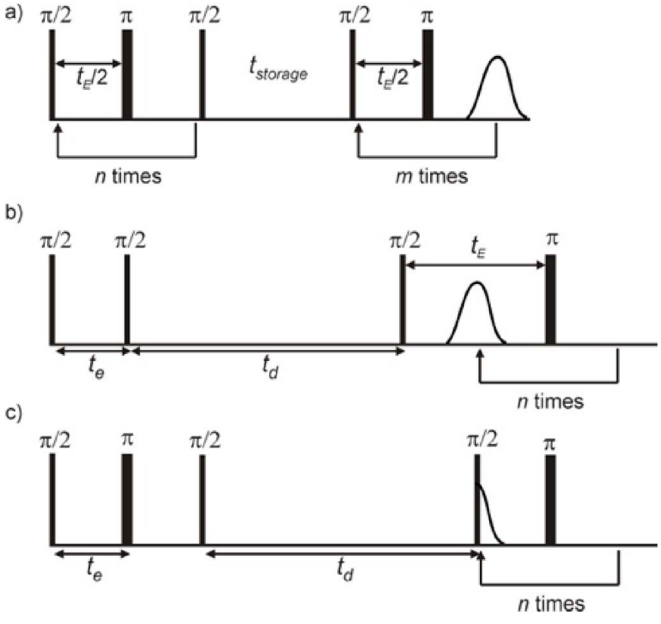

Fig. 1. a) T_2-T_2 pulse sequence for the measurement of transverse relaxation exchange. t_E is the echo time, n and m are the numbers of echoes used in the indirect and direct dimension respectively. b) Stimulated echo sequence. c) Reference DDIF sequence followed by a CPMG, t_e is the encoding time and t_D is the time for the molecules to diffuse, t_E is the echo time and n the number of echoes in the CPMG.

The encoding time t_e should satisfy the weak encoding limit, that means that the magnetization modulation has a wavelength comparable to the pore size. In that regime, the modulated magnetization from the DDIF truly reflects the spatial pattern of the internal field and consequently, the pore shape [24]. The DDIF signal decays with a characteristic time which, in the case of spherical pores, can be rescaled to obtain the diameter d by:

$$d = \pi\sqrt{D\tau} \tag{2}$$

The 2D sequence is achieved by applying a CPMG pulse train for signal detection. In order to remove the longitudinal relaxation from the DDIF signal $E(t_d, NT_E)$, a reference sequence (Fig. 1c) is performed and the reference signal, $R(t_d, NT_E)$, recorded. The subtraction of the reference signal from the echo signal with a correction factor a_0 $S(t_d, NT_E) = E(t_d, NT_E) - a_0 R(t_d, NT_E)$, eliminates relaxation effects on the stimulated echo attenuation. The factor a_0 is obtained as the ratio E/R in the limit of large t_d. As in the T_2-T_2 experiment, and after the rescaling according to Eq. (2), a 2D map can be generated through numerical inversion.

3. Experimental

3.1. Polymeric network

Polymer beads with hierarchical pore structure of ethylene glycol dimethacrylate and 2-hydroxyethyl methacrylate [poly(EGDMA-*co*-HEMA)] were synthesized as previously reported [17]. The synthesis was carried out at 85°C in a 250mL round-bottom flask equipped with a reflux condenser and a magnetic stirrer on a water bath for 2h. To obtain 10g of dry polymer, a molar ratio of 3.0:1.0:9.3:250 of HEMA (6.2mL), EGDMA (3.2mL), cyclohexane (17.2mL), and water (77.0mL) was used in the reaction at a stirring speed of 450rpm. For the suspension polymerization, reaction cyclohexane was used as a porogenic agent, poly(vinyl pyrrolidone) (PVP) as a suspension stabilizer and benzoyl peroxide (BPO) was used as a radical initiator. The amount of cross-linker used was 33mol % giving, as a result, a polymeric network with a porosity approximately 84%.

The resulting system consists of hierarchically distributed pore sizes. These systems present high stability, maintaining the pore structure even in the dry state. Because of the hydrophilic characteristic of these materials, polar solvents can swell the network, which modifies its pore structure. To reach the full swelling of the network, small samples of polymer beads were immersed in a vial containing distilled water at room temperature for 24h. After that 75mg of sample were extracted from the vial and gently placed in a 5mm outer diameter NMR sample tube.

The pore size distribution was previously reported for both the dry and swollen state using mercury intrusion [17] and the DDIF sequence [20] respectively. Both results are in a good agreement taking into account the effect of swelling. Three different pore populations in the

range of 10–100μm were distinguished.

3.2. NMR measurements

The experiments were carried out at 25°C using a Magritek Kea2 spectrometer operating at 60MHz for ^{1}H. A 1.4T permanent magnet (Varian EM360) was used. For the T_2-T_2 map, the echo time t_E was set to 0.5ms and 8000 echoes in the direct dimension while 32 logarithmically spaced point, from 1 to 8000 echoes, were acquired in the indirect dimension, the storage time was set to 500ms and 64 scans were added. CPMG echo times were varied from 0.3ms to 1ms without appreciable influence due to diffusion.

In the DDIF sequence, the encoding time $t_e = 0.5$ms was chosen to guarantee that the weak encoding limit is reached (a linear behaviour was observed up to 2ms) and the characteristic decay times can be related to the pore size by Eq. (2) [24]. The diffusion time t_d was varied from 0.5ms to 4s in 32 logarithmically increased steps and the echo time for the CPMG was set to $t_E = 0.5$ms, 16 scans were added both in DDIF as in the reference sequence due to the phase cycling needed for the latter one. A diffusion coefficient $D = 2.3 \times 10^{-9}$m^2/s for bulk water at 25°C was used [25].

4. Results and discussion

4.1. T_2-T_2 experiments

In Fig. 2a the T_2-T_2 exchange map for a storage time $t_{storage} = 500$ms is shown. Numerical inversion was performed by using the adaptive truncation of matrix decompositions introduced by Teal and Eccles [26]. Three diagonal peaks are clearly identified at values $T_2 = 260$, 40 and 4ms. The diagonal peaks are attributed to each of the three different porous populations previously described for this hierarchical porous system [18]. The high connectivity of the pore network is evidenced by the presence of off-diagonal peaks that correlate all of the diagonal ones. A complete analysis of molecular migration as a function of the storage time is out of the scope of this work and will be presented elsewhere. For the purpose of this work, it suffices to note that 500ms of storage time is in of the same order as the diffusion times used for the DDIF encoding and that the system is completely correlated in this period.

4.2. DDIF-CPMG experiment

According to the procedure depicted in the theoretical section, the DDIF sequence was applied in the 2D fashion and the signals $E(t_d, NT_E)$ and $R(t_d, NT_E)$ recorded during a CPMG acquisition. Upon rescaling, the signal $S(t_d, NT_E)$ is obtained, and the corresponding d-T_2 map is shown in Fig. 2b. Three regions of pore sizes are assigned to the system; pore 1 (P_1) corresponds to a distribution of pore sizes between 85μm and 125μm, pore 2 (P_2) ranges between 20μm and 40μm and pore 3 (P_3) between 10μm and 20μm. The projections in both directions are in agreement with the 1D data shown in a previous work [20], i.e. three clearly distinct pore sizes and the corresponding T_2 values. Two distinct features are present, indicated by arrows in Fig. 2b, which are not commonly observed in most d-T_2 maps reported in the literature. These peaks could be accounted for if there were two pores of the same characteristic length, but with very different liquid/surface interactions, however these would contradict previous results of water evaporation [18,19]. Therefore, these cross-peaks could be attributed to molecular exchange between the cavities P_1 and P_2, occurring within the diffusion time, as observed in the T_2-T_2 experiment.

The question that arises is how to obtain the information on the surface relaxivity parameter from this data set. Liu et al. [14] have estimated the surface relaxivity ρ_2 from the d-T_2 experiment by calculating the mean value of T_2 for each pore length in the 2D map. As a result, they obtained monotonic relationships between pore length and

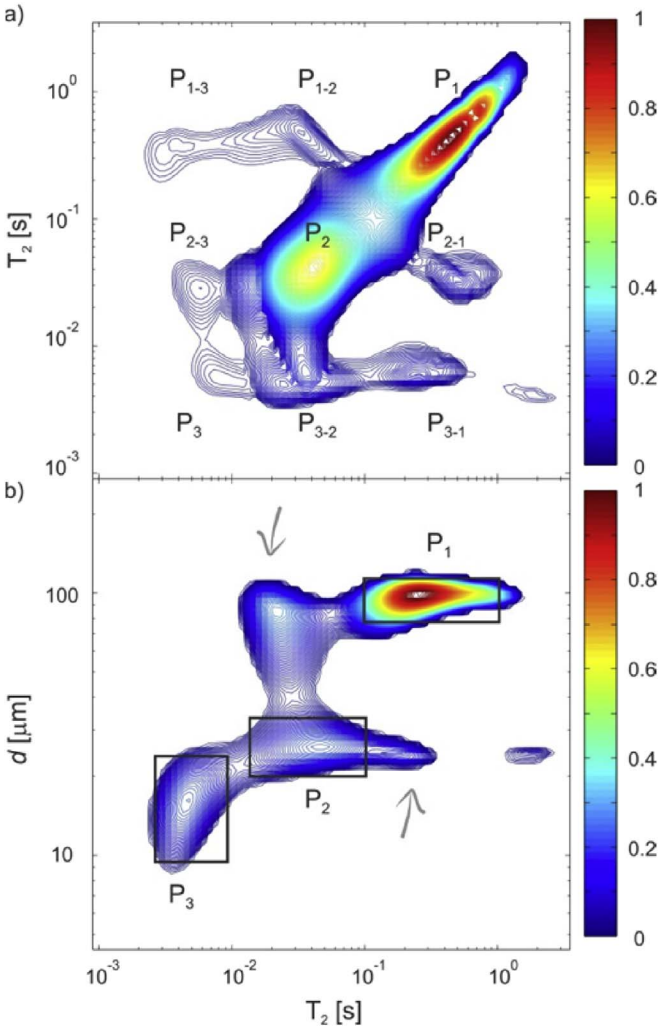

Fig. 2. a) 2D T_2-T_2 exchange map. Main diagonal peaks correspond to non-migrant fluid in the network, while the off-diagonal contributions represent the water molecules migrating among different T_2 environments. The storage time is 500ms.b) d-T_2 correlation map. The arrows indicate exchange peaks and the rectangles the projection area used to construct Fig. 3.

T_2 values in the pore regions. From the slope of the $d(T_2)$ curve the effective surface relaxivities of rock samples were extracted, according to Eq. (1), where the $S/V = 6/d$ ratio for spherical cavities was assumed. In Fig. 3a the same analysis was performed in our data, where the different environments are represented with different symbols for the sake of clarity. It is clear that this data cannot be interpreted as linearly related to the surface relaxivity over the whole system. Therefore, each pore environment was analysed separately by integration over the ranges represented by rectangles in Fig. 2b and the results are plotted in Fig. 3b–d. For each pore population, the pair (d,T_2) for the maximum value was used to calculate $\rho_2 = \frac{d}{6T_2}$, and the linear function $d = 6\rho_2 T_2$ is plotted as a dotted red line. This linear relationship represents the behaviour of confined water in the fast diffusion regime, for a single relaxivity parameter. By excluding the exchange peak from the analysis, the curves for the smaller and larger cavity size ranges present a monotonic behaviour, as expected. However, the central pore size distribution (Fig. 3c), especially for sizes over 30μm cannot be correctly analysed. It should be noticed that this region is the more affected by the presence of the exchange peaks, evidencing that the non-monotonic dependence of d with T_2 shown in Fig. 3a arises from this contribution. It must be mentioned that different data inversion software were tested, a systematic variation of the regularization parameters carried out and integration over different regions of the 2D

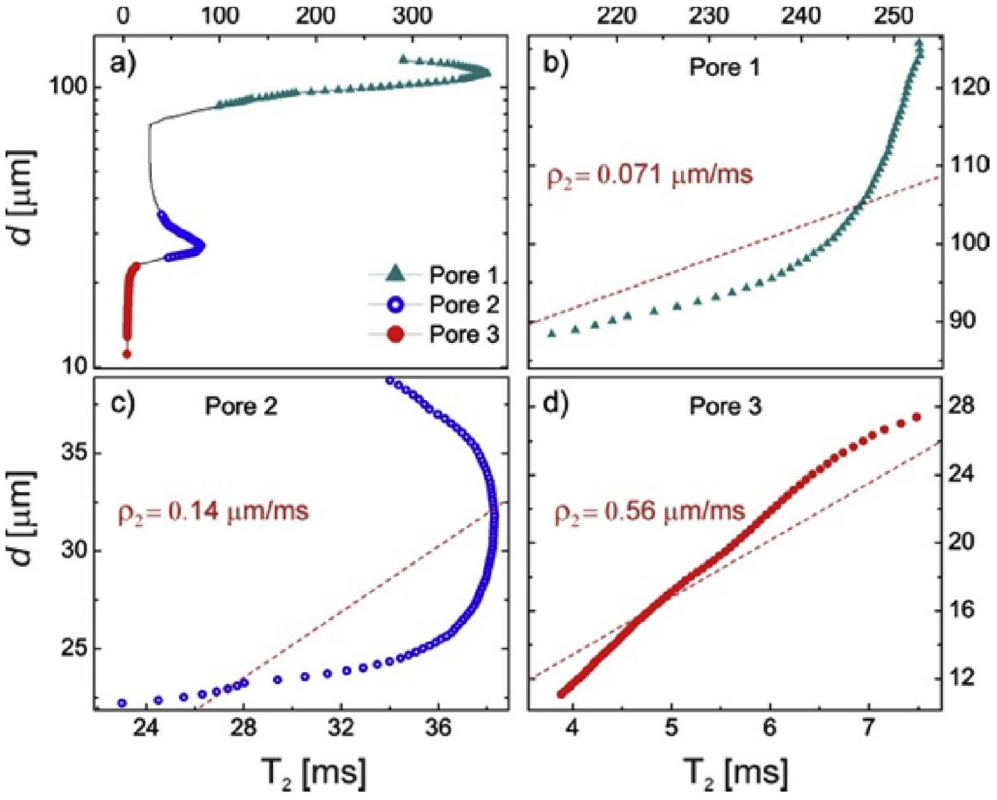

Fig. 3. Pore length as a function of T_2 mean value by integrating over the a) complete 2D map of Fig. 2b, b) P_1 region, c) P_2 region and d) P_3 region. The dashed line represents the behaviour due in the fast diffusion limit for the maximum amplitude in the d-T_2 map.

maps carried out, always with similar results. While in most inorganic porous media, a unique surface relaxivity parameter is found for each pore size [11,14]. For the reported cavity sizes the fast diffusion regime should be reached, thus in the studied polymeric systems ρ_2 changes not only from pore to pore, but also within the same cavity. In a recent study [20] we probed the liquid surface interaction for each pore size as a function of the polymer network cross-linker content, by combination of 1D experiments. For these systems, an increase in cross-linker content renders a decrease in OH groups. We observed an increase of superficial OH groups only in the smaller cavity sizes for low cross-linker content. However, a prediction of the distribution of the HEMA monomers cannot be carried out a priori. The experiments presented here extend our previous knowledge by recognizing a heterogeneous distribution of OH groups within each cavity, leading to a heterogeneous surface relaxivity in each pore.

5. Conclusions

The molecular exchange between different environments in a porous system with a hierarchical distribution of pore sizes was shown by means of a T_2-T_2 experiment, and the system is very well connected for a storage time of 500ms. This time is representative of the diffusion time used in a 2D d-T_2 experiment, where exchange peaks were observed for the first time. Even though this system is an ideal candidate for probing such phenomenon, extreme care must be taken in the analysis of simpler systems, where in principle this behaviour was not expected. We have shown that the data analysis is complex, and a region where the validity of $d(T_2)$ must be defined a priori in order to infer information on the surface relaxivity. Remarkably, the 2D experiment reveals that the behaviour of the surface relaxivity in organic porous systems is extremely dependent on the structural formation and the information obtained from the pore length-relaxation correlation could aid in the exploration of different synthetic routes in order to tune desired material properties.

Acknowledgments

We thank Cesar Gomez and Miriam Strumia for sample preparation. We would like to acknowledge the financial support received from CONICET, ANPCYT (PICT-2010-2274) and SeCyT-UNC.

References

[1] J.G. Seland, K.E. Washburn, H.W. Anthonsen, J. Krane, Phys. Rev. E - Stat. Nonlinear, Soft Matter Phys. 70 (2004) 1–10.
[2] S.M. Islam, K. Tuhina, M. Mubarak, P. Mondal, J. Mol. Catal. A Chem. 297 (2009) 18–25.
[3] F.M. Plleva, I.Y. Galaev, B. Mattiasson, J. Sep. Sci. 30 (2007) 1657–1671.
[4] P.T. Callaghan, Translational Dynamics and Magnetic Resonance: Principles of Pulsed Gradient Spin Echo NMR, Oxford University Press, Oxford, 2011.
[5] Y.-Q. Song, S.G. Ryu, P.N. Sen, Nature 406 (2000) 178–181.
[6] K.R. Brownstein, C.E. Tarr, J. Magn. Reson 26 (1977) 17–24.
[7] H.Y. Carr, E.M. Purcell, Phys. Rev. 94 (1954) 630.
[8] S. Meiboom, D. Gill, Rev. Sci. Instrum. 29 (1958) 688–691.
[9] A.P. Cocco, G.J. Nelson, W.M. Harris, A. Nakajo, T.D. Myles, A.M. Kiss, J.J. Lombardo, W.K.S. Chiu, Phys. Chem. Chem. Phys. 15 (2013) 16377–16407.
[10] S. Muncaci, C. Mattea, S. Stapf, I. Ardelean, Magn. Reson. Chem. 51 (2013) 123–128.
[11] Z.-X. Luo, J. Paulsen, Y.-Q. Song, J. Magn. Reson 259 (2015) 146–152.
[12] M.D. Hürlimann, K.G. Helmer, L.L. Latour, C.H. Sotak, J. Magn. Reson. Ser. A 111 (1994) 169–178.
[13] R.W. Mair, G.P. Wong, D. Hoffmann, M.D. Hurlimann, S. Patz, L.M. Schwartz, R.L. Walsworth, Phys. Rev. Lett. 83 (1999) 3324–3327.
[14] H. Liu, M.N. d'Eurydice, S. Obruchkov, P. Galvosas, J. Magn. Reson. 246 (2014) 110–118.
[15] R.T. Lewis, J.G. Seland, J. Magn. Reson 263 (2016) 19–32.
[16] R.T. Lewis, K. Djurhuus, J.G. Seland, J. Magn. Reson 259 (2015) 1–9.
[17] C.G. Gomez, G. Pastrana, D. Serrano, E. Zuzek, M. a. Villar, M.C. Strumia, Polym. Guildf. 53 (2012) 2949–2955.
[18] E.V. Silletta, M.I. Velasco, C.G. Gómez, R.H. Acosta, M.C. Strumia, G.A. Monti, Langmuir 30 (2014) 4129–4136.
[19] M.I. Velasco, E.V. Silletta, C.G. Gomez, M.C. Strumia, S. Stapf, G.A. Monti, C. Mattea, R.H. Acosta, Langmuir 32 (2016) 2067–2074.
[20] E.V. Silletta, M.I. Velasco, C.G. Gomez, M.C. Strumia, S. Stapf, C. Mattea, G.A. Monti, R.H. Acosta, Langmuir 32 (2016) 7427–7434.
[21] P. McDonald, J.-P. Korb, J. Mitchell, L. Monteilhet, Phys. Rev. (2005) E 72.
[22] K. Washburn, P. Callaghan, Phys. Rev. Lett. 97 (2006).
[23] L. Venkataramanan, Y.Q. Song, M.D. Hürlimann, IEEE Trans. Signal Process 50 (2002) 1017–1026.
[24] Y.Q. Song, Concepts Magn. Reson. Part A (2003) 97–110.
[25] M. Holz, S.R. Heil, A. Sacco, Phys. Chem. Chem. Phys. 2 (2000) 4740–4742.
[26] P.D. Teal, C. Eccles, Inverse Probl. 31 (2015) 45010.